Supporting Information

Title (A Novel 3D Porous Pseudographite/Si/Ni Composite Anode Materials Fabricated by a Facile method)

Weiming Su[a,b], Ruchao Wan[a,b], Yue Liang [a,b], Yinze Zuo[a,b]* and Yuefeng Tang[a,b,c]*

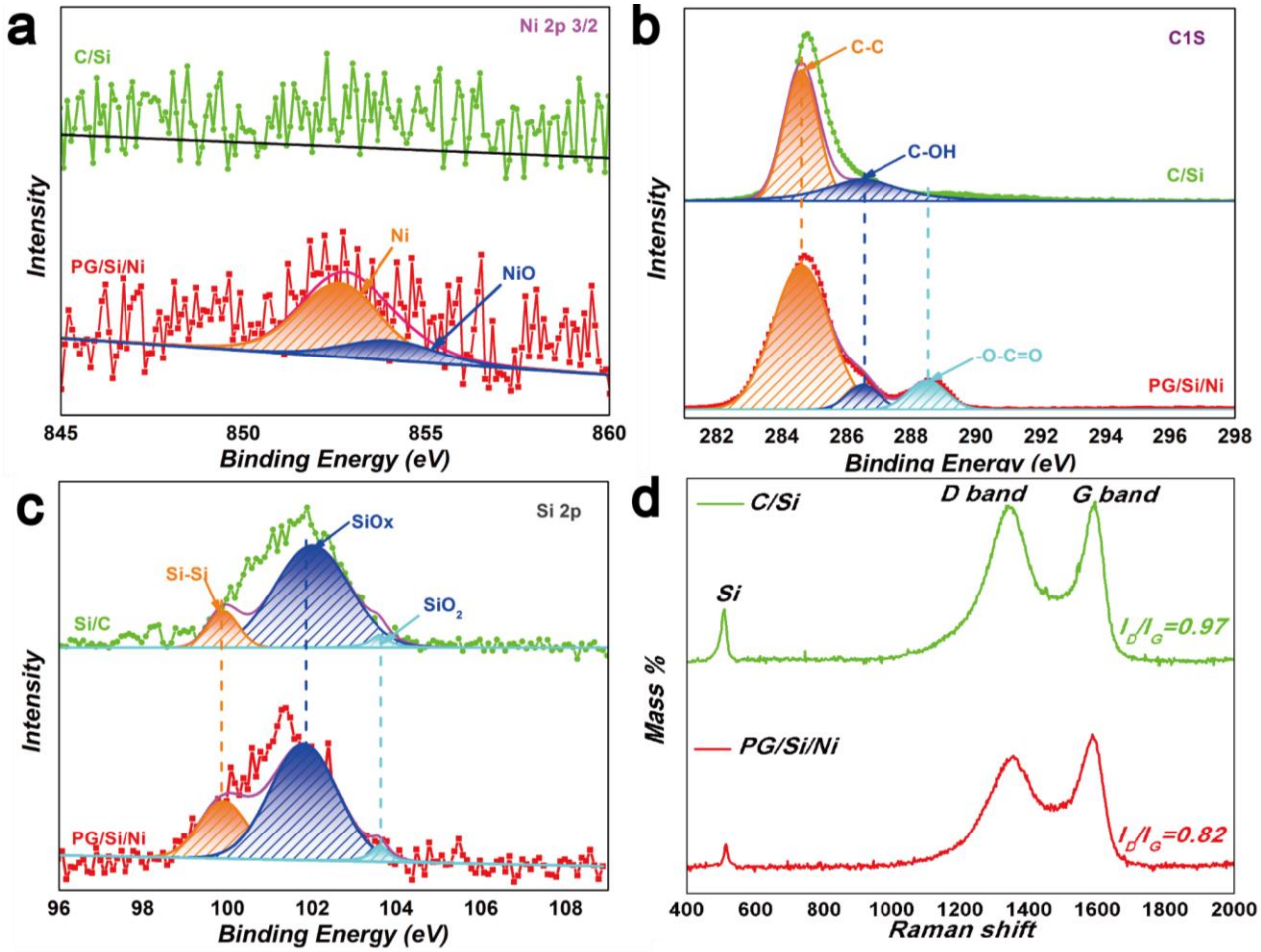

Fig. S1. High-resolution XPS spectra of the C/Si and PG/Si/Ni: (a) Ni 2p3/2, (b) Si 2p,

(c) C 1s, (d) Raman spectra of the C/Si and PG/Si/Ni composite.

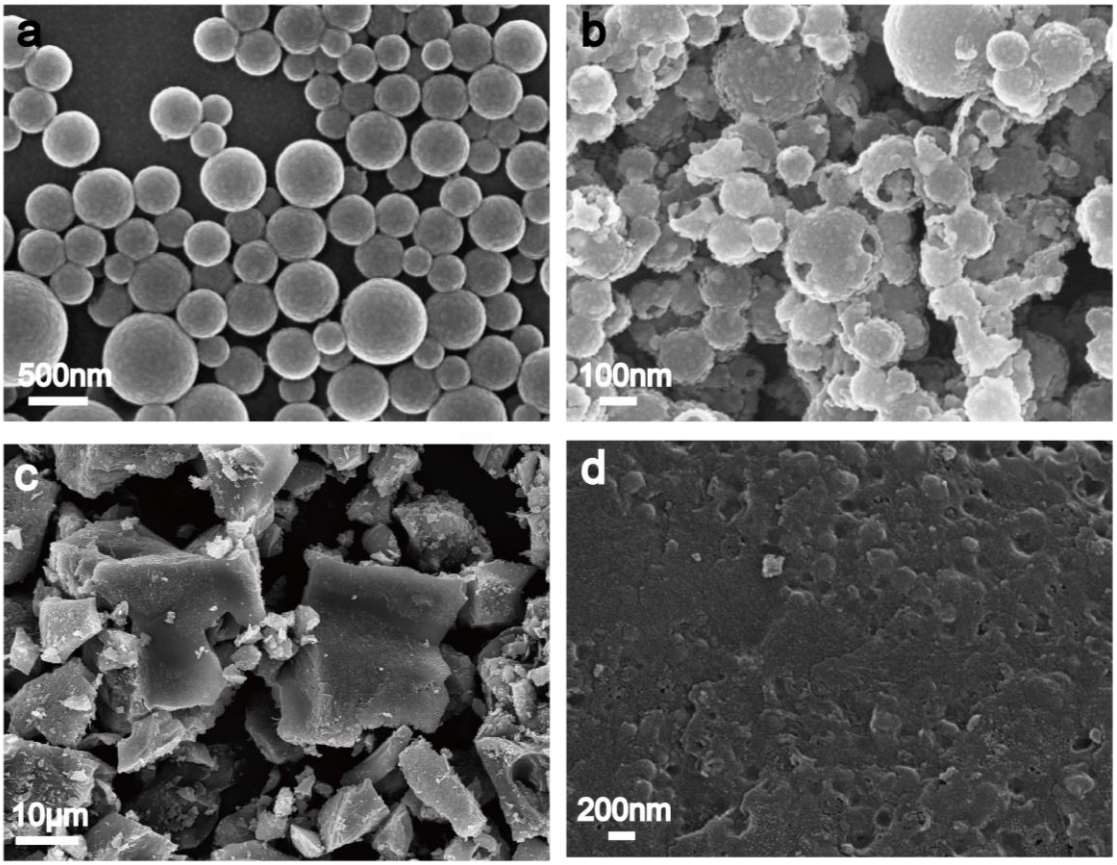

Fig. S2. SEM images of (a) as-prepared SiO_2 nanospheres. (c) as-prepared Si nanospheres. (b,c) C/Si composite.

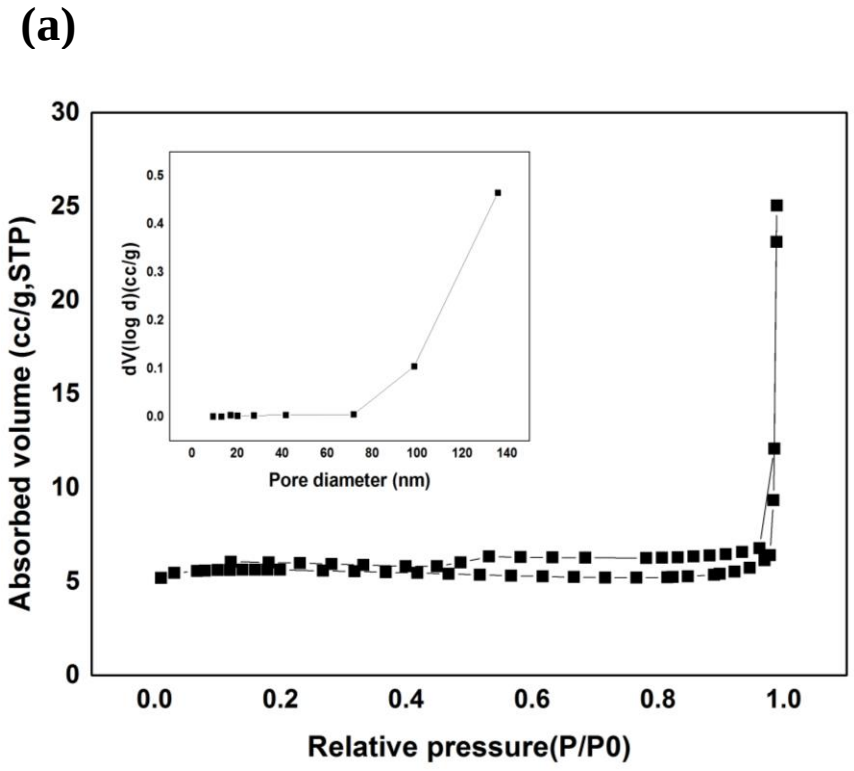

(b)

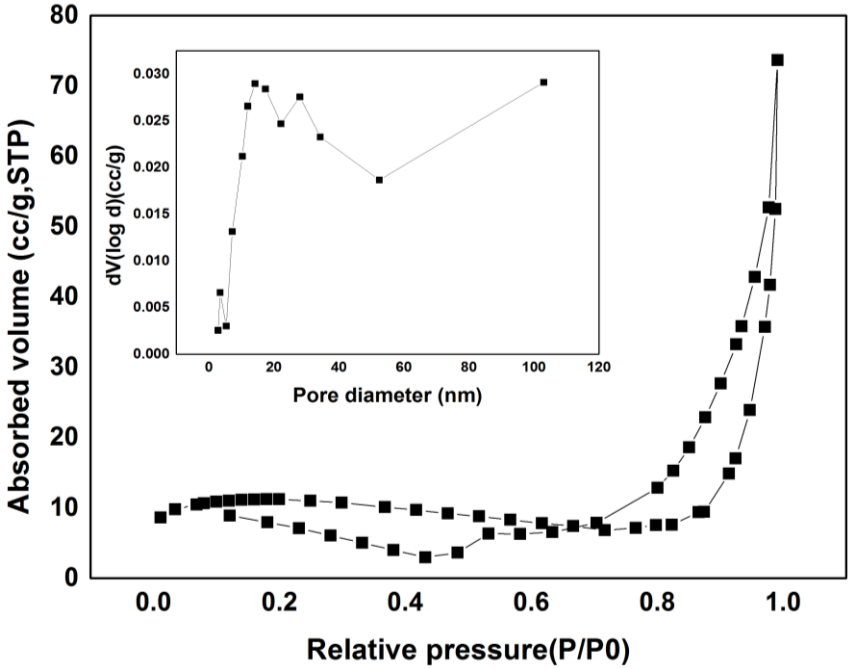

Fig. S3. N_2 adsorption–desorption isotherms of samples: (a) C/Si, (b) PG/Si/Ni. The inset in each figure shows the relevant pore size distribution calculated by the BJH formula.

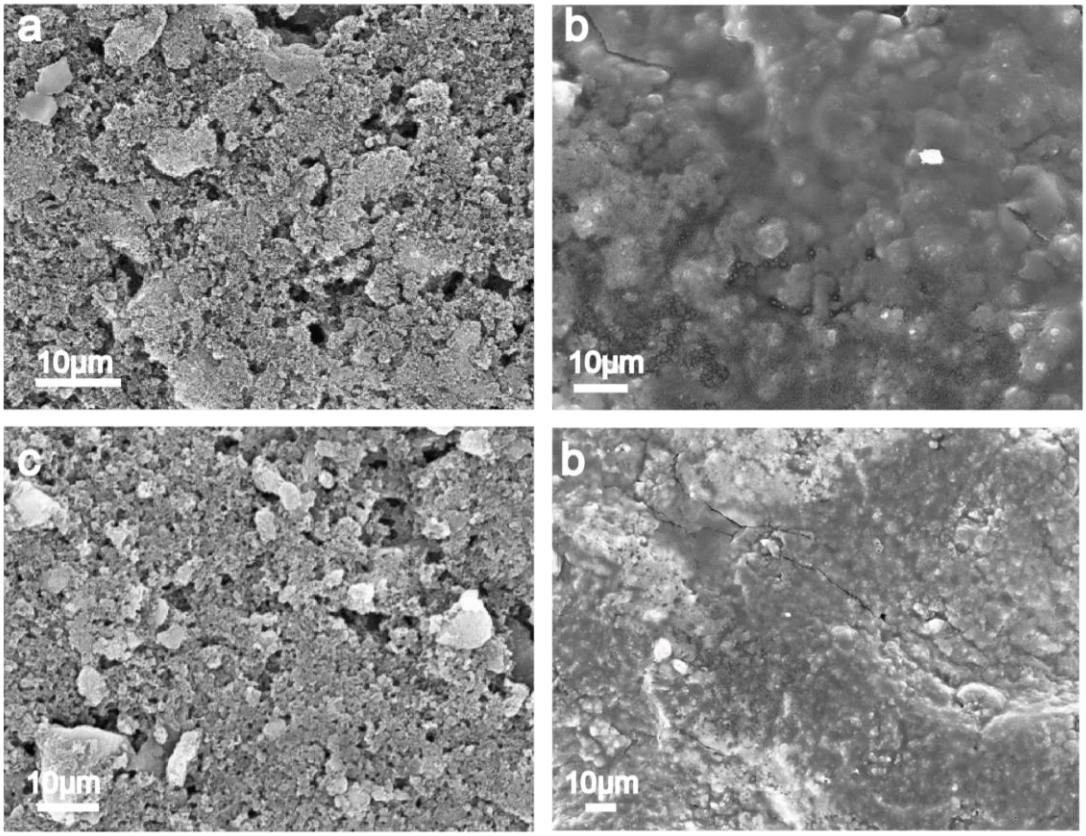

Fig. S4. SEM images of C/Si composite, (a) before cycling, and (b) after 2000 cycles; SEM images of PG/Si/Ni hybrid composite, (c) before cycling and (d) after 2000 cycles.

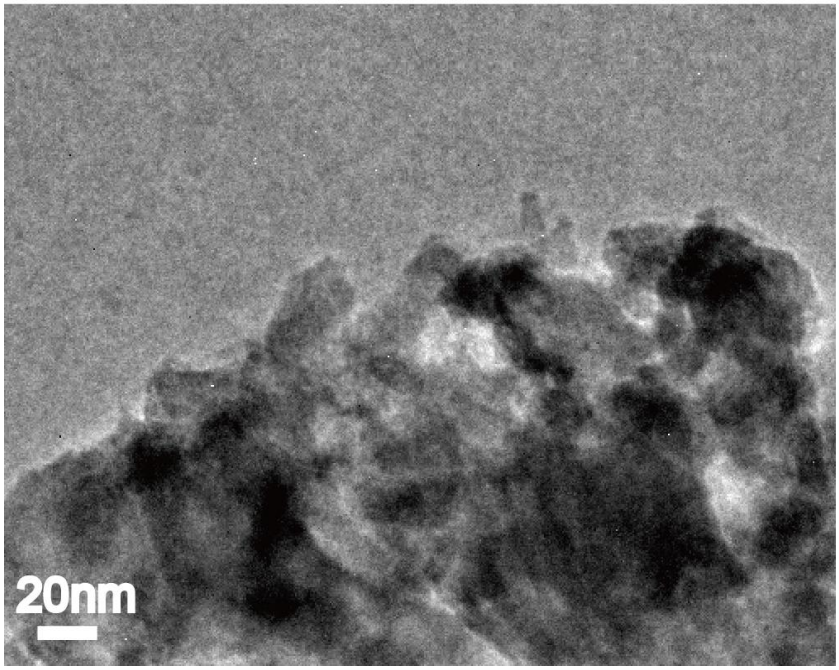

Fig. S5 TEM image of the Ni distribution.

Table S1. N_2 adsorption-desorption isothermal analysis of C/Si and PG/Si/Ni.

Sample	$D_{average}$ (nm)	Surface $Area_{total}$ (m^2/g)
C/Si	64.4	16.9
PG/Si/Ni	19.3	79.8

Table S2. Fitting results of cells with C/Si and PG/Si/Ni as anodes

Sample	Rs [Ω]	Rct [Ω]	W
C/Si	25.35	1923	3497
PG/Si/Ni	3.887	321	499